Available online at www.sciencedirect.com
SCIENCE DIRECT®
PERGAMON
International Journal of Heat and Mass Transfer 46 (2003) 4703–4715
International Journal of HEAT and MASS TRANSFER
www.elsevier.com/locate/ijhmt

Evaporation of water by free or mixed convection into humid air and superheated steam

C. Debbissi [a], J. Orfi [b,*], S. Ben Nasrallah [c]

[a] Institut Préparatoire aux Etudes d'Ingénieurs de Monastir, Avenue Ibn Eljazzar, 5019 Monastir, Tunisie
[b] Département de Physique, Faculté des Sciences de Monastir, Avenue Ibn Eljazzar, 5019 Monastir, Tunisie
[c] Département d'Energétique, Ecole Nationale d'Ingénieurs de Monastir, Avenue Ibn Eljazzar, 5019 Monastir, Tunisie

Received 14 February 2001; received in revised form 6 January 2003

Abstract

This paper concerns a numerical analysis of the evaporation of water in pure air, humid air and superheated steam in an externally insulated channel. Results were obtained for mixed and free convection driven by combined thermal and mass buoyancy forces. For natural convection case, the analysis is restricted to situation in which combined buoyancy forces act in the downward direction. The results show that below a certain temperature of the free stream, water evaporation rate decreases as the humidity of air increases and above it this relation reverses. This temperature "inversion point temperature" was treated in previous experimental and numerical studies in the case of forced convection. In this work, particular attention is paid to study the effect of the ambient conditions on evaporation rate of water and the inversion temperature phenomenon in the condition of free and mixed convection.

1. Introduction

The evaporation of liquids in air is important in heat and mass transfer and exists in different industrial applications such as drying, air conditioning and desalting. The case of evaporation of water by superheated steam has also received considerable attention in many theoretical and experimental studies [1–10]. Because the using of the superheated vapour steam as drying medium is recommended for drying materials that are sensitive to oxidation and sensitive temperature such as food products. Also superheated vapour as a dehydrating medium contains no contaminants, it poses no threat to nutrias product safety. Thus, the use of superheated vapour reduces the loss of nutritional value during the drying process [4,6].

Wenzel and White [1] and Chu et al. [2] were the first to show experimentally that more evaporation occurs in superheated vapour than in air. Since then, the change in drying rate with the gas flow humidity and the estimation of inversion temperature values has been the subject of various theoretical and experimental investigations. Schwartze and Bröcker [7] present a comparative table summarising some of previous results giving the inversion temperature which varies between 433.15 and 533.15 K depending on study approach (theory or experiment) and on flow characteristics (turbulent or laminar).

The first experimental investigation leading to find the inversion temperature was carried out by Yoshida and Hyŏdŏ [3]. They reported an inversion point temperature (between 433.15 and 449.15 K) for an equipment of countercurrent water and air, flowing a wetted wall column. Chow and Chung presented the first numerical studies of the evaporation of water into dry air and superheated steam for a laminar [4] and turbulent [6] forced convection over a flat plate. Their analysis showed that below the called inversion point temperature of the free stream, the evaporation rate is less effective as the stream humidity rises and beyond this temperature the opposite is true. Wu et al. [5] developed

* Corresponding author. Tel.: +216-3-500-511; fax: +216-3-500-514.
E-mail addresses: jamel.orfi@fsm.znu.tn (J. Orfi), sassi.bennasrallah@enim.rnu.tn (S. Ben Nasrallah).

0017-9310/$ - see front matter © 2003 Elsevier Ltd. All rights reserved.
doi:10.1016/S0017-9310(03)00092-9

Nomenclature

C	mass fraction of water vapour
c_p	specific heat at constant pressure [J kg^{-1} K^{-1}]
c_{pa}	specific heat for air [J kg^{-1} K^{-1}]
c_{pv}	specific heat for water vapour [J kg^{-1} K^{-1}]
d	channel width [m]
D	mass diffusivity [m^2 s^{-1}]
e	factor equal to zero for forced convection and unity for free and mixed convection case
g	gravitational acceleration [m s^{-2}]
H	channel length [m]
i	grid point index number in the flow direction
I	upper grid point index number in x-direction
j	grid point index number in transverse direction
J	upper grid point index number in y-direction
L_v	latent heat of evaporation [J kg^{-1}]
$\dot{m}$	evaporating mass flow [kg s^{-1} m^{-2}]
M_a	molecular weight of air [kg mol^{-1}]
M_v	molar mass of vapour [kg mol^{-1}]
Nu_m	interfacial mean Nusselt number
Nu_x	peripheral local Nusselt number
p	pressure of the moist air in the channel [N m^{-2}]
p_g	motion pressure (dynamic pressure) [N m^{-2}]
p_v	partial pressure of vapour [N m^{-2}]
p_{vs}	partial pressure of saturated vapour [N m^{-2}]
p_0	ambient pressure [N m^{-2}]
Rev	average evaporating rate [kg m^{-2} s^{-1}]$^{0.5}$
Sh_m	mean Sherwood number
Sh_x	peripheral local Sherwood number
T	absolute temperature [K]
T_i	interfacial temperature [K]
T_w	dry wall temperature [K]
u	axial velocity [m s^{-1}]
v	transverse velocity [m s^{-1}]
w	relative humidity, p_v/p_{vs} [%]
x	coordinate in the axial direction [m]
x^*	dimensionless axial coordinate
y	coordinate in the transverse direction [m]

Greek symbols

β	volumetric coefficient of thermal expansion, $-1/\rho(\partial\rho/\partial T)_{p,C}$, [K^{-1}]
β^*	volumetric coefficient of expansion with mass fraction, $-1/\rho(\partial\rho/\partial C)_{p,T}$
λ	thermal conductivity of the fluid [W m^{-1} K^{-1}]
μ	dynamic viscosity of the fluid [kg m^{-1} s^{-1}]
ρ	density of the fluid [kg m^{-3}]

Subscripts

1	wet plate
2	dry plate
0	ambient condition

a numerical model to study the effectiveness of superheated steam, humid air, and dry air as dehydration media for wedge-shaped food products. They presented numerical results for different combinations of fluid temperature, mass ratio, and specimens wedge angle. Authors reported also that an inversion point in the evaporation rate occurs around 548.15 K.

Recently Schwartze and Bröcker [7] carried out a theoretical study of the evaporation of water into its own vapour, air and a mixture thereof. They introduced refined definitions of the inversion point temperature. They defined firstly a local inversion temperature as a temperature at which the evaporation rates from an infinitesimal area for two gas flows with different vapour mole fractions is equal. Then, they defined the apparent inversion temperature as the temperature at the beginning of evaporation area for which average evaporation rate into two gas flows with different vapour mole fractions is equal. These new and precise definitions enable a more precise description of the inversion temperature phenomenon and permit to explain the variation of the inversion temperature values obtained in earlier studies.

The physical reason for the existence of the inversion point temperature has been reported in several previous studies [4–10]. Chow and Chung [4] presented an interesting explanation where only the heat transfer was taken into account. Their reasoning is based on the temperature depression between the water interface and the gas flow as well as the variation of fluid properties by changing the ambient conditions. Schwartze and Bröcker [7] explain the existence of the inversion temperature by considering heat and mass transfer in the evaporation process.

It can be noted that all mentioned theoretical studies dealing with the evaporation of water into air and mixture and superheated steam were generally conducted in the forced convection flow (see for example [4,7,8]). Evaporation of liquids by free convection driven by thermal and mass buoyancy forces into air is treated by different authors (see for example [13,14,17]).

Yan and Lin [15] presented a numerical analysis to investigate the effects of the latent heat transfer, in association with the evaporation into air of a finite liquid film on the channel wall, on the free convective heat and mass transfer. Recently Debbissi et al. [18] investigated

numerically the coupled heat and mass transfers by natural convection during water evaporation into air in a vertical heated channel by including radiative heat transfer between plates. They observed that the evaporative cooling disturbs considerably the velocity and temperature profiles in particular near the exit section of the channel. The axial distributions of the relative sensible, latent and radiative heat fluxes are presented for different ambient conditions. The interfacial mass flux at the channel exit is presented as function of inlet temperature and for various ambient humidity and pressure.

At our knowledge the inversion temperature in the case of evaporation by free convection is not studied. The main objective of this work is to extend the study of the evaporation of water into air, mixture and superheated vapour to the free and mixed convection flows. A particular attention will be addressed to the inversion temperature in the free and mixed convection regimes.

2. Analysis

The present work deals with a numerical analysis of evaporation of water into hot humid air and superheated steam by mixed and natural convection induced by the thermal and mass buoyancy forces in a finite vertical channel (Fig. 1). The studied channel is made up of two parallel plates. The first plate is externally insulated and wetted by an extremely thin water film while the second one ($y = d$) is dry and isothermal. The imposed temperature is maintained at $T_w = 100$ °C for all computations. For natural convection case, the moist air in the ambient is driven into the channel by the resultant

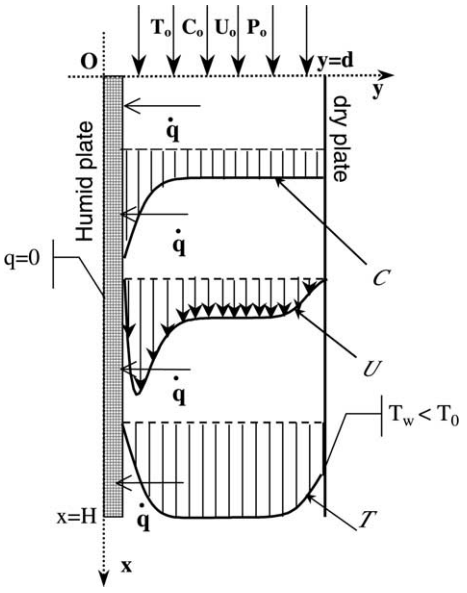

Fig. 1. Physical description of the system.

forces of thermal and solutal buoyancies. Since wet wall is insulated, its interfacial temperature is approximately equal to wet bulb temperature, which is always considered, less than that of ambient stream. Thus, the thermal buoyancy force near this surface acts downwards and the gas flow moves in this direction. For the dry wall maintained at uniform T_w less than the ambient temperature ($T_0 > 100$ °C) air is aided by the buoyancy force of heat transfer to move downward [14,15]. Finally, one can note that since the wet plate is externally insulated, the energy required for evaporation comes entirely from ambient stream.

For mathematical formulation of the problem, the following simplifying assumptions are taking into consideration:

- the liquid film is assumed to be extremely thin. Under this assumption, transport in the liquid film can be replaced by approximate boundary conditions for gas flow [13],
- the boundary layer approximations are generally used to study the downward flow in the channel induced by natural convection,
- the viscous dissipation and the pressure work are negligible,
- the Dufour and Soret effects are negligible,
- the thermal radiation is negligible,
- ideal gas law is used for humid air and superheated vapour.

The heat and mass transfer for the laminar mixed or free convection induced by the combined thermal and mass buoyancy forces, with the usual boundary layer approximation, can be described by the following governing equations [12,18]:

Continuity equation

$$\frac{\partial \rho u}{\partial x} + \frac{\partial \rho v}{\partial y} = 0 \tag{1}$$

x-momentum equation

$$u\frac{\partial u}{\partial x} + v\frac{\partial u}{\partial y} = -\frac{1}{\rho}\frac{\mathrm{d}P}{\mathrm{d}x} - e(\beta g(T - T_0) + \beta^* g(C - C_0)) + (1/\rho)\frac{\partial}{\partial y}\left(\mu\frac{\partial u}{\partial y}\right) \tag{2}$$

Energy equation

$$u\frac{\partial T}{\partial x} + v\frac{\partial T}{\partial y} = \frac{1}{\rho c_p}\left[\frac{\partial}{\partial y}\left(\lambda\frac{\partial T}{\partial y}\right) + \rho D(c_{pv} - c_{pa})\frac{\partial T}{\partial y}\frac{\partial C}{\partial y}\right] \tag{3}$$

Species diffusion equation

$$u\frac{\partial C}{\partial x} + v\frac{\partial C}{\partial y} = \frac{1}{\rho}\frac{\partial}{\partial y}\left(\rho D\frac{\partial C}{\partial y}\right) \tag{4}$$

$e(\beta g(T-T_0)+\beta^* g(C-C_0))$ represents the momentum transfer caused by the combined buoyancy forces. This term is zero (i.e. $e=0$) for the pure forced convection case.

The second term in the right side of the energy equation presents the energy transport through the inter-diffusion of species.

Thermo-physical properties of gas mixture are considered as variable with temperature and composition. The correlations used in this study were given in [13] for viscosity, mass heat capacity and mass diffusion coefficients and in [16] for thermal conductivity.

In this study of steady mixed or free channel flow, the overall mass balance described by the following equation should be satisfied at every axial location:

$$\int_0^d \rho u(x,y)\,\mathrm{d}y = \mathrm{d}\rho_0 u_0 + \int_0^x \rho v(x,0)\,\mathrm{d}x \tag{5}$$

Boundary conditions

* At $x=0$:
  - $u=u_0$, $T=T_0$, $C=C_0$,
    For the free convection case, one must add:
  - $$P(x=0) = -\frac{1}{2}\rho u_0^2 \quad \text{and} \quad P(x=H)=0; \tag{6}$$

* At $y=0$ (isolated plate):
  - $u=0$;
  - the transverse velocity of gas is deduced by assuming that the air–water interface is semipermeable:

$$v(x,0) = \frac{-D}{1-C(x,0)}\left.\frac{\partial C}{\partial y}\right|_{y=0} \tag{7a}$$

  - the energy balance at the insulated interface ($y=0$) is evaluated by

$$-\lambda\frac{\partial T}{\partial y} - \frac{\rho L_v D}{1-C(x,0)}\frac{\partial C}{\partial y} = 0 \tag{7b}$$

  - According to Dalton's law and by assuming the interface to be at thermodynamic equilibrium and the air–vapour mixture is an ideal gas mixture, the concentration of vapour can be evaluated by

$$C(x,0) = \frac{M_v/M_a}{p/p_{vs} + M_v/M_a - 1} \tag{7c}$$

p_{vs} is the equilibrium pressure of vapour given by the following equation [19]:

$$\log_{10} p_{vs} = 28.59051 - 8.2\log T + 2.4804\times 10^{-3}T - 3142.32/T \tag{7d}$$

* $y=d$ (the isothermal plate):
  - $u=0$, $v=0$, $T=T_w$
  - the impermeability of the dry plate ($y=d$) to the water vapour can be described by

$$\frac{\partial C}{\partial y} = 0 \tag{7e}$$

The governing equations for the evaporation of water into its own vapour were obtained by adjusting the above equations. In this case, the species equation and the associated boundary conditions, which become irrelevant, were ignored. Also the second term in the right side of the energy equation (Eq. (3)) and the buoyancy term of the mass diffusion in the momentum equation (Eq. (2)) are suppressed. Finally, the equation giving interfacial transverse velocity is expressed as

$$v(x,0) = \frac{1}{\rho L_v}\left.\frac{\partial T}{\partial y}\right|_{y=0} \tag{8}$$

In order to describe the mass and energy magnitude transported between the channel walls and moist air, the following dimensionless coefficients are used [11,20]:

- The peripheral local Nusselt number is defined as

$$Nu_x = \frac{h_x 2d}{\lambda} = -\frac{2d[(\partial T/\partial y)_{y=0}]_x}{T(x,0)-T_m} \tag{9a}$$

  where, h_x is the local heat transfer coefficient.
  T_m is the fluid bulk temperature at a cross section:

$$T_m = \int_0^d \rho u\cdot T\,\mathrm{d}y \Big/ \int_0^d \rho u\,\mathrm{d}y \tag{9b}$$

- The mean Nusselt number is

$$Nu_m = \frac{1}{x}\int_0^x Nu_x\,\mathrm{d}x \tag{9c}$$

- Similarly and for mass transfer, the mean Sherwood number is defined as

$$Sh_m = \frac{1}{x}\int_0^x Sh_x\,\mathrm{d}x \tag{9d}$$

  where Sh_x is the local Sherwood number defined by

$$Sh_x = -\frac{2d[(\partial C/\partial y)_{y=0}]_x}{C(x,0)-C_m}, \tag{9e}$$

  C_m is the fluid bulk concentration.
- The average evaporated mass flux is given by

$$\bar{\dot{m}} = \frac{1}{H}\int_0^H \rho v(x,0)\,\mathrm{d}x \tag{10a}$$

- The evaporating rate of water, commonly used in the previous studies [4,5,7,10], is expressed as

$$R_{ev} = \frac{10^4\bar{\dot{m}}}{\sqrt{\rho_0 u_0/H}} \tag{10b}$$

3. Solution method

The presented system of Eqs. (1)–(5) is solved numerically using finite difference method. The flow area is divided into a regular mesh placed in axial and transverse direction and a (71,71) grid is retained in actual computations. A fully implicit marching scheme where the axial convection terms were approximated by the upstream difference and the transverse convection and diffusion terms by the central difference, is employed to transform the governing equations into finite difference equations. The resolution of the obtained algebraic equations was marched in downstream direction since flow under consideration is a boundary layer type.

For a given thermal and mass boundary conditions, the solution procedure is briefly outlined as following:

Step 1 Guess an arbitrary velocity u_0 (which is the inlet known velocity in the case of mixed convection).

Step 2 For the given axial location i, guess the wetted wall temperature T^* and solve the finite difference form of species equation.

Step 3 Solve the finite difference form of energy equation and compare the new value T of wetted temperature to T^* by testing if

$$\left|\frac{T(i,1)-T^*(i,1)}{T(i,1)}\right| < 10^{-6}$$

If this criteria is not satisfied, return to (2) and modify the wetted wall temperature by using the bisection method.

Step 4 Guess a pressure P^* at the i axial location and solve the momentum and continuity finite difference equations, then verify the satisfaction of the overall conservation of mass expressed by the following criteria:

$$\left|\int_0^d \rho u(x,y)\,\mathrm{d}y - \left(\mathrm{d}\rho_0 u_0 + \int_0^x \rho v(x,0)\,\mathrm{d}x\right)\right| \Big/ (\mathrm{d}\rho_0 u_0) < 10^{-6}$$

Step 5 If this condition is not satisfied, return to step 4 and modify the pressure value P^* and repeat the steps (2–4).

Step 6 For free convection case, test if the exit dynamic pressure is zero, else return to (1) and modify the inlet velocity by using bisection method.

To ensure that results were grid independent, the solution was obtained for different grid sizes for typical case program test. Table 1 shows that the differences in the evaporative rate obtained using 71×71 and 201×101 grids are always less than 2%.

To check the adequacy of the numerical scheme adopted in the present study, different limiting cases for laminar forced convection were considered. The results for the case of forced convective heat and mass transfer inside a channel have been treated with constant physical properties. The channel is made up of two parallel plates. The first plate is isothermal and impermeable. The second is insulated and kept at constant concentration. The procedure have been tested by comparing the present results for mean Nusselt number Nu_m at the isothermal wall to those of Mercier et al. found in Shah and London [11]. Similarly the mean Sherwood Sh_m at insulated plate is compared to the analytical solution by employing heat and mass transfer analogy [11]. The results of this first comparison presented in Fig. 2 show a good agreement for heat and mass transfer coefficients.

Table 1
Comparison of the evaporating rate of water for various grid arrangements

Grid size	Rev: $C_0 = 0.25$	Rev: $C_0 = 0.75$
31×31	1.686	1.500
71×71	1.679	1.494
101×71	1664	1.483
201×101	1.654	1.474

Furthermore, the comparison is carried out for the case of forced combined heat and mass transfer in a channel made up by a humid insulated plate and the other one is kept at the ambient temperature. The physical properties of humid air flow are considered to be variable. The numerical code has been tested successfully by comparing the present solutions for the rate of evaporation R_{ev} with the results of Hassan et al. [8] who studied the problem of evaporation by forced convection over a flat plate (see Fig. 3).

Finally, results for evaporation by natural convection in a heated channel was validated in a former paper [18]. Through these program tests, the present numerical algorithm is considered to be suitable to study the present problem.

4. Results and discussion

This work includes two sections. The first one concerns mixed convection flow. The effect of ambient conditions on the development of velocity, temperature and concentration profiles as well as on the characteristics of heat and mass transfer is investigated. The results for evaporative rate of water from wetted plate in a parallel stream of air and humid air are also presented in this part. The second section studies the free convection case. All the above cases are based on a vertical channel with length of 1 m and width of 0.05 m. Moreover, the dry wall temperature is always kept at $T_w = 373.15$ K which is less than ambient gas temperature so that the thermal buoyancy force acts in the downward direction.

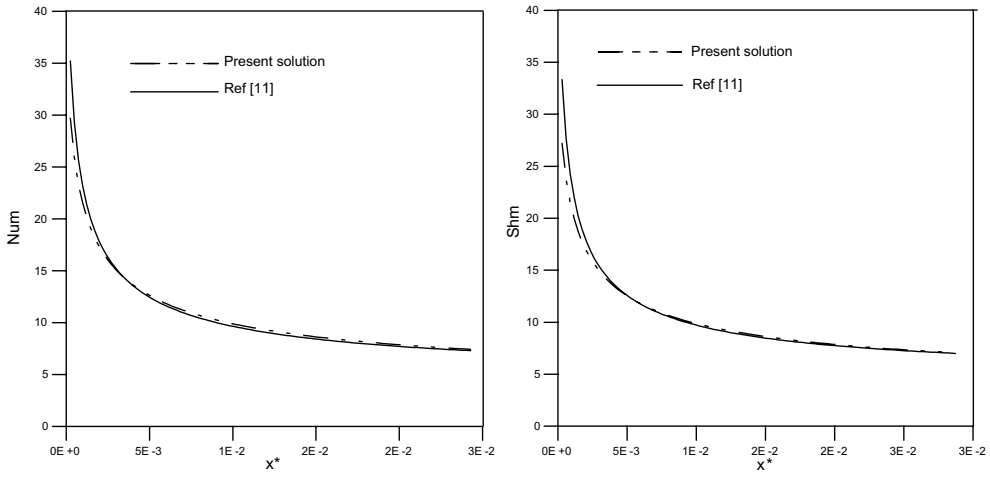

Fig. 2. Axial evolution of heat and mass coefficients.

4.1. Evaporation in mixed convection flows

Figs. 4–6 show the effects of the inlet velocity, temperature and concentration on the development of the axial velocity, temperature and concentration profiles. It is seen that velocity profiles of moist air at the channel entrance is uniform. They become distorted as the flow moves downstream and keep decreasing at the centreline. This result can be justified by the fact that in conformity with the larger buoyancy force through thermal diffusion, maximum velocity is noted near channel walls and meanwhile to reduce the velocity at the centre to maintain the overall mass balance. The influence of rising the inlet velocity on the shape of the axial profile is significant as indicated in Fig. 4a and b. It is apparent that the flow field is less distorted for higher inlet velocity indicating that the secondary flow induced by the combined effect of thermal and mass buoyancy forces becomes negligible compared to the forced convection effect.

Fig. 4c gives the temperature distribution inside the channel. Profiles show a development of two thermal boundary layers with smaller temperature obtained near the walls. Under the present condition of adiabatic evaporation and the small pressure deflect in the flow, the temperature of humid plate is slightly constant along the wall.

The gas flow near the humid plate is cooled especially at the channel inlet because of the amount of the energy needed to water evaporation. For the thermal boundary conditions considered here, this amount of energy is supplied by the gas flow through the loss of sensible heat. The inspection of Fig. 4c and d in the central region of the channel shows that the temperature profiles exhibit a maximum, which approaches the value of the inlet temperature for higher inlet velocity.

Concentration profiles are presented in Fig. 4e and f. They indicate a rapid development of mass boundary layer. Because of the almost invariance of the wetted wall temperature (Fig. 4c and d), the water vapour concentration of fluid adjacent to this wall is nearly constant as indicated in plots. Also, a care examination of Fig. 4e and f shows that increasing the inlet velocity reduces the thickness of mass boundary layer.

The effect of the ambient temperature on the axial velocity, temperature and concentration profiles at the mid-section ($x/H = 0.5$) are shown in Fig. 5. As seen in Fig. 5a, a little increasing in interfacial temperature accompanied by important thermal gradients near plates are noted when T_0 increases. Fig. 5c illustrates that if the ambient temperature goes higher, both the concentration and mass gradients at the humid wall increase. This behaviour is in conformity with the fact that energy needed for water evaporation comes entirely from the gas. Therefore a higher T_0 induced more water evaporation. Fig. 5b gives the axial velocity profile at $x = H/2$ for various inlet temperature. It is seen that increasing in T_0 leads to an acceleration of the fluid adjacent to the plates indicating the larger buoyancy force through thermal diffusion. Fig. 6 illustrate the changing behaviours of velocity, temperature and concentration profiles in transverse direction for the location ($x = H/2$) with a variation of ambient humidity. As foreseen, the major effect of C_0 is noted for concentration profiles (Fig. 6c). For temperature and velocity profiles, Fig. 6a and b indicate that no significant change occurs near the dry wall. Whereas near the humid one, an increasing of C_0 induces a decreasing of the temperature gradient at this interface. Therefore, the thermal buoyancy force is reduced and the maximum velocity of the fluid adjacent the humid wall slows down.

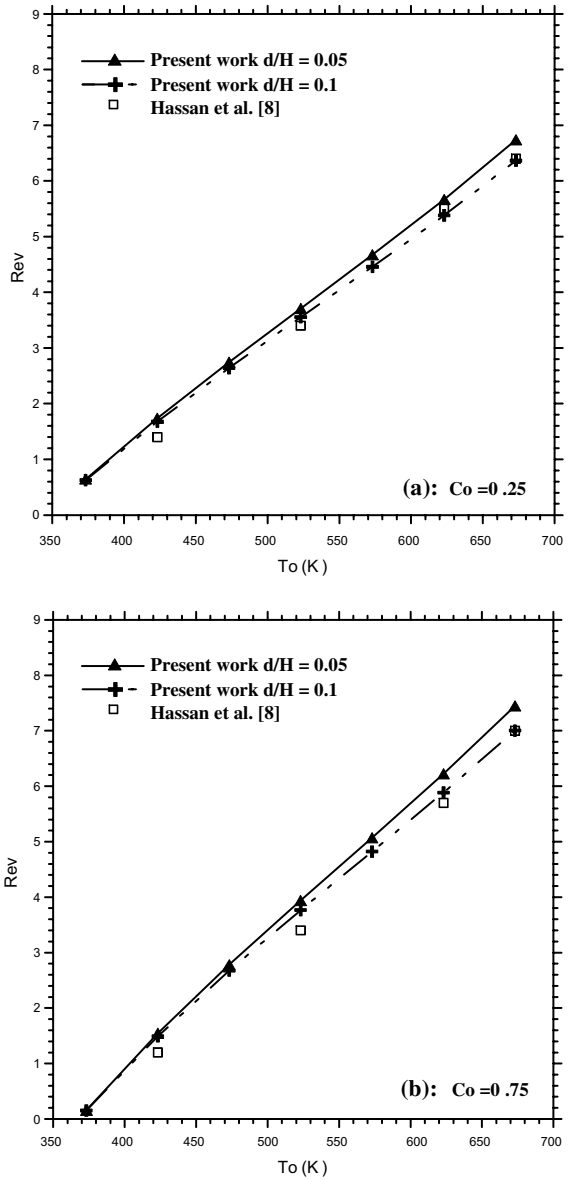

Fig. 3. Variation of the evaporating rate with the inlet temperature.

Attention is now turned to the evaporative rate into a stream of humid air or superheated steam. The variations of the evaporation rates as function of free stream temperature under various ambient concentrations are reported in Fig. 7a for the same free stream mass flux. For lower ambient temperature Fig. 7a shows the generally accepted fact that water evaporates faster in air than in moist air. This result reverses for a higher T_0 where the evaporation rate is greater in the case of a steam than that of a humid air. The evaporation rates for dry air and superheated steam converged as the free stream temperature approaches the value of 479.15 K. This value is within 3% higher than that obtained by Schwartze and Bröcker [7]. For more comprehensive explanation of the inversion temperature existence by considering the heat and mass transfer, evaporative rate is plotted versus the free stream concentration and presented for various ambient temperatures in Fig. 7b.

The existence of inversion temperature is due to the existence of opposing effects favouring evaporation in different conditions:

- effects decreasing with vapour concentration; among these effects, we cite temperature potential $(T_i - T_0)$ effect (T_i increases with vapour concentration and consequently $(T_i - T_0)$ decreases). These effects dominate when the ambient temperature is below to the inversion temperature,
- effects increasing with vapour concentration; we cite for example the latent heat effect (the latent heat L_v decreases with vapour concentration). These effects dominate when the ambient temperature is higher than the inversion temperature.

These opposing effects are counterbalanced at the inversion temperature.

In Fig. 8, the evaporative rates of water into air and humid air under various humidities are plotted versus the free stream temperature. Results were reported for both cases of forced ($e = 0$) and mixed ($e = 1$) convection. It can be seen from Fig. 8a that for higher inlet velocity (mass flow rate), the buoyancy forces have no effects on the rate of evaporation. Whereas at lower inlet mass flow rate, a significant variation occurs by taking into consideration the thermal and mass buoyancy effects. This result is clearly seen in Fig. 8b and c especially for smaller air humidity. In this situation, interfacial temperature T_i is relatively small (Fig. 6a). Therefore, the thermal buoyancy force is intensified and by the way fluid adjacent to the humid wall is accelerated (Fig. 6b). These effects cause a water evaporation enhancement.

4.2. Evaporation in natural convection flows

In this section attention was paid to the evaporation of water by natural convection driven by the simultaneous presence of combined buoyancy effects of heat and mass diffusion. Development of the axial velocity is plotted in Fig. 9a. It is seen that velocity profiles remain uniform at the entrance region. Further downstream, the buoyancy effects perturb considerably the flow field. The shape of flow field is analogous to that obtained for mixed convection case with a small inlet velocity (Fig. 4a). The maximum velocity is obtained near the humid plate where the buoyancy force is more pronounced.

Seen in Fig. 9b, is the axial evolution of the gas stream temperature. At $y = d$, the temperature is constant along

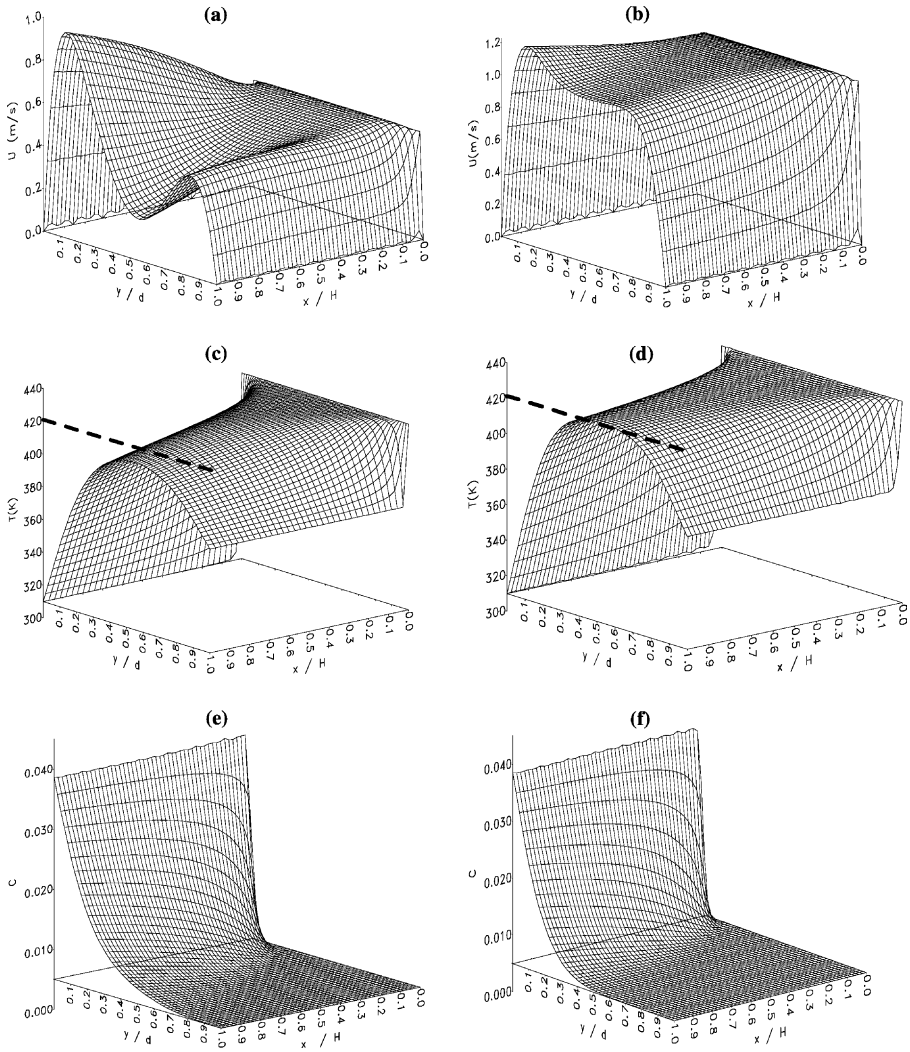

Fig. 4. Development of flow, thermal and mass fields: effects of inlet velocity (mixed convection case) ($T_0 = T_w = 373.15$ K, $C_0 = 0.005$, $d/H = 0.05$, $p_0 = 1$ atm, $u_0 = 0.5$ for a, c, e and $u_0 = 1$ for b, d, f).

the wall according to the imposed boundary condition ($T = T_w$). Also for $y = 0$ the plots indicate that the humid wall temperature $T(x, 0)$ remains constant. This result confirms the reasonable simplifying assumption used in [4,8] saying that the interfacial temperature $T(x, 0)$ is constant along the water surface. Furthermore, it is apparent that the temperature of the fluid close to the wet wall decreases monotonically with y from its maximum value at the channel centre to reach $T(x, 0)$. This implies that the direction of sensible heat needed for evaporation is from the flow to the interface. Consistent with the wet bulb temperature invariability and according to the relation (7c), Fig. 9c indicates that the interfacial vapour concentration is almost uniform along the wetted wall interface.

Fig. 10a and b display the evolutions of pressure deflect along the channel with vapour concentration at fixed free stream temperature of 443.15 K (for Fig. 10a) and 593.15 (for Fig. 10b). It is seen that the pressure deflect ($-p_g$) increases first to reach a maximum value near the channel entrance. Beyond this location it decreases to reach the boundary condition $p_g = 0$ at $x = H$. By comparing Fig. 10a and b, one can observe that higher inlet temperature T_0 correspond to a larger pressure deflect. This result can be justified by the important thermal diffusion driving force that occurs for hot mixture. Whereas, the higher in free stream mass vapour concentration leads to a higher in buoyancy force of mass diffusion which acts upward then the flow is retarded and the pressure deflect goes lower. Finally,

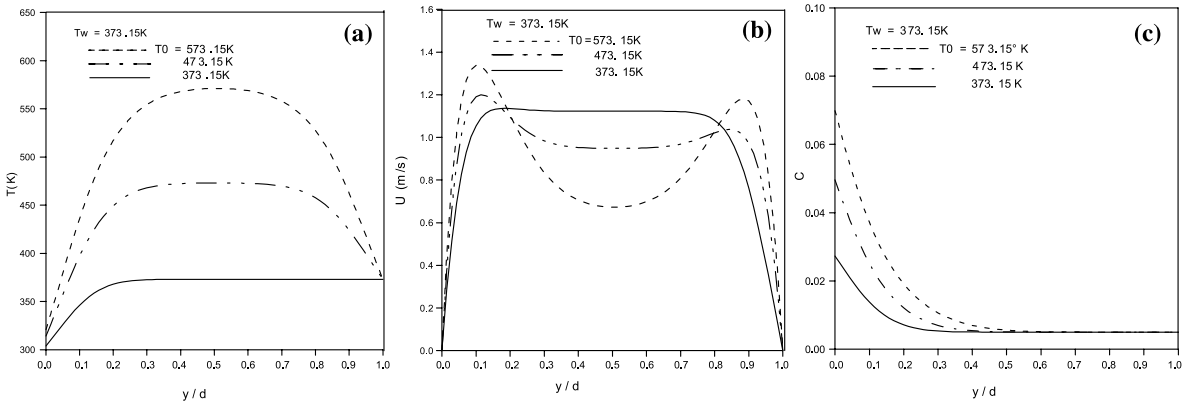

Fig. 5. Effect of ambient temperature on temperature, axial velocity and concentration ($T_w = 373.15$ K, $C_0 = 0.005$, $d/H = 0.05$, $p_0 = 1$ atm, $u_0 = 1\ \mathrm{m\,s^{-1}}$).

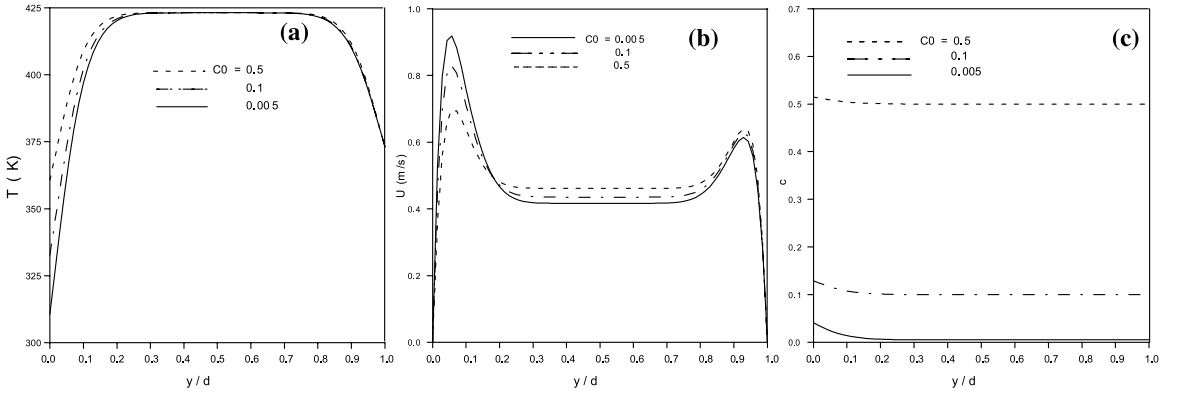

Fig. 6. Effect of ambient humidity on temperature, axial velocity, and concentration ($T_0 = 423.15$ K, $T_w = 373.15$ K, $d/H = 0.05$, $p_0 = 1$ atm, $u_0 = 0.5\ \mathrm{m\,s^{-1}}$).

the general observation for all curves is that pressure deflect is always negligible compared to the atmospheric pressure. One point worth mentioning is that the pressure deflect in the flow resulting from the combined buoyancy forces is small enough so that humid interface is similar to be at atmospheric pressure.

Fig. 11 presents the effect of the mass vapour concentration and temperature of the free stream on the inlet flow rates. The evolution of the flow rate is a direct consequence of the above-discussed variation of pressure deflect with T_0 and C_0. As seen from figure, the higher inlet flow rate is found to be associated with a larger T_0 at fixed vapour concentration or lower C_0 at imposed free stream temperature.

Before studying the effect of the ambient conditions of temperature and concentration on the evaporative rate in the case of natural convection, some previous results dealing with the evaporation by forced convection needed to be mentioned. The first result concerns the effect of inlet mass flux on the evaporation rate. It is verified experimentally by Haji and Chow [10] and analytically by Chow and Chung [6] that the scaled expression of water evaporation rate into both air and steam is independent on free stream mass flux. This result is confirmed in the present study by comparing Fig. 8a–c for forced convection case ($e = 0$). The second result seen on these curves is the small variation of the inversion temperature with varying the mass flow rate. This result is in contrast with the finding of [7].

As these results, one could foresee the existence of an inversion temperature in the case of natural convection where the inlet flow rate depends on the ambient conditions of temperature and concentration. Fig. 12a illustrates the existence of an inversion temperature close to 473.15 K. Below this value, water evaporates faster in air than in vapour stream. Whereas above this temperature, water evaporates faster in stream.

The change in evaporation rate when free stream varies from dry air to pure vapour at 423.15, 473.15 and 623.15 K is shown in Fig. 12b. This figure shows clearly

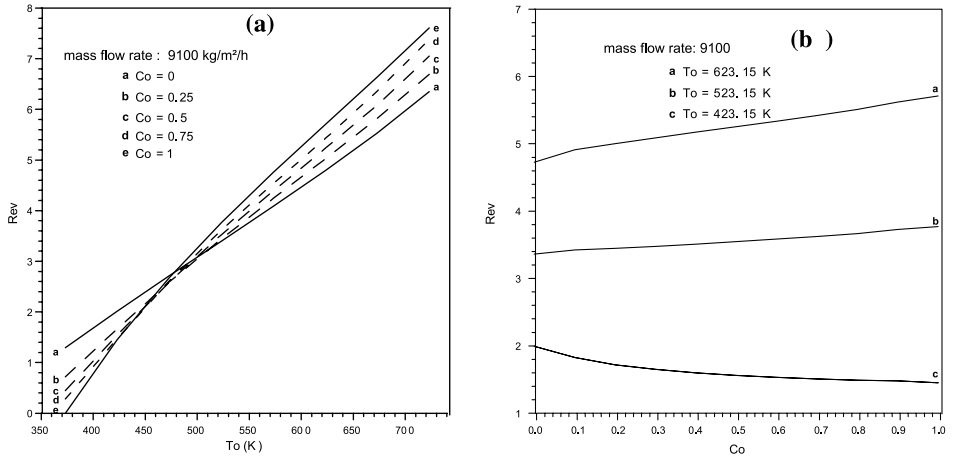

Fig. 7. Influence of ambient conditions on the evaporation rate ($T_w = 373.15$ K, $d/H = 0.05$, $p_0 = 1$ atm).

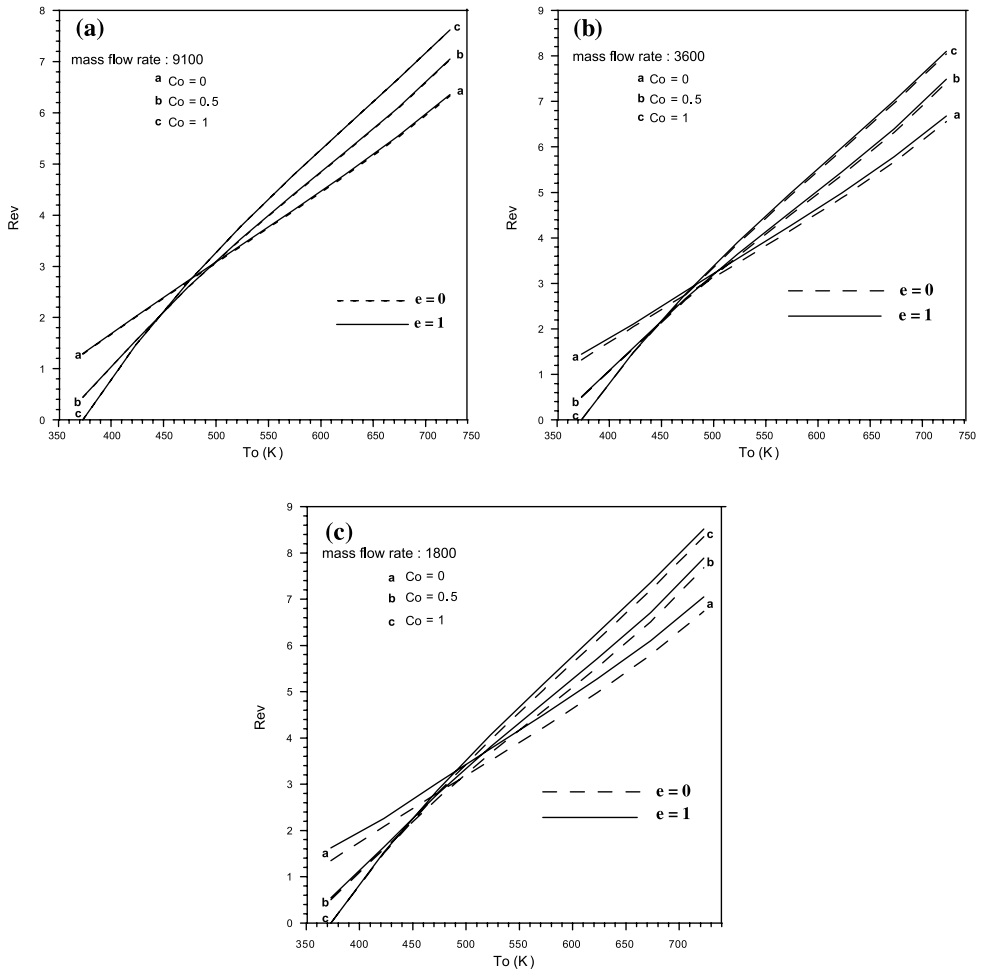

Fig. 8. Effect of inlet mass flow rate on the evaporation rate ($T_w = 373.15$ K, $d/H = 0.05$, $p_0 = 1$ atm).

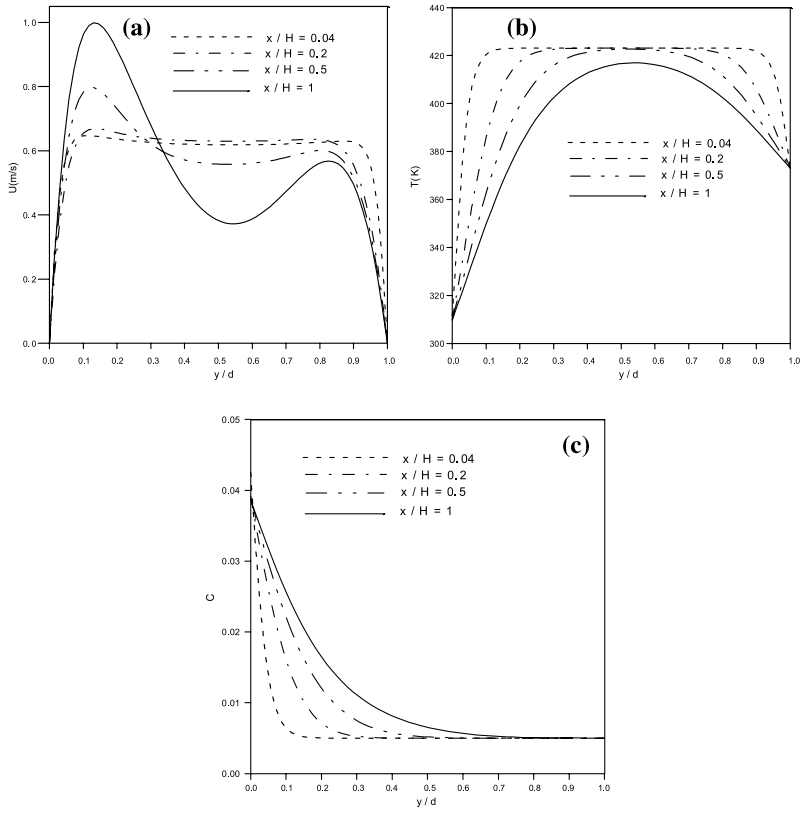

Fig. 9. Evolution of axial velocity temperature and concentration natural convection case ($T_0 = 423.15$ K, $T_w = 373.15$ K, $C_0 = 0.005$, $d/H = 0.05$, $p_0 = 1$ atm).

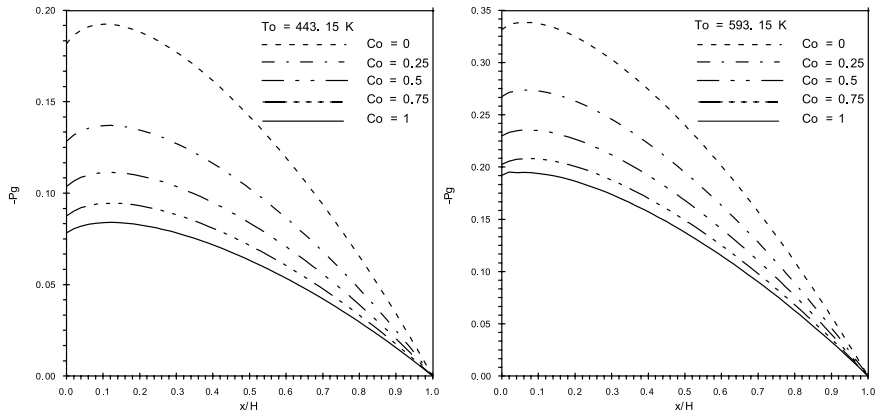

Fig. 10. Effect of inlet temperature and concentration on axial distribution of motion pressure ($T_w = 373.15$ K, $C_0 = 0.005$, $d/H = 0.05$, $p_0 = 1$ atm).

that at the temperature of inversion the evaporation rate is slightly constant (at less than 4%) inspite of the increase in vapour concentration. For low temperature ($T_0 = 423.15$ K) the evaporation rate declines as the stream humidity rises. Inversely, for high temperature ($T_0 = 623.15$ K) the evaporation is more effective as the free mass vapour concentration increased.

Fig. 13 illustrates the numerical results for the mean humid surface temperature versus vapour mass concentration for different free stream temperatures. The

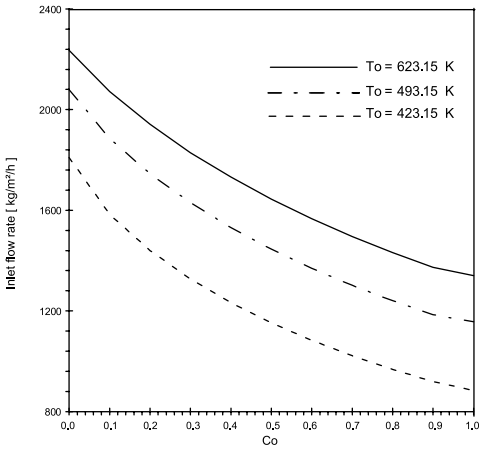

Fig. 11. Effect of inlet temperature and concentration on inlet masse flow rate ($T_w = 373.15$ K, $d/H = 0.05$, $p_0 = 1$ atm).

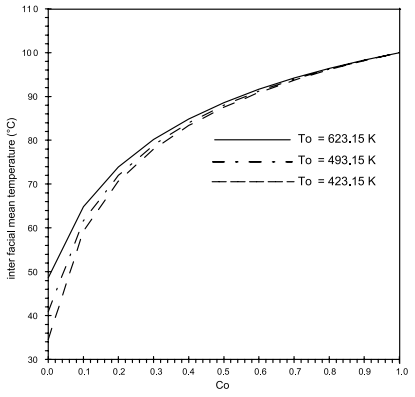

Fig. 13. Effect of ambient conditions on mean wall temperature ($T_w = 373.15$ K, $d/H = 0.05$, $p_0 = 1$ atm).

figure shows that wetted surface temperature varies appreciably at lower C_0. In this case a mixture with higher temperature results in a higher interfacial temperature for the same C_0. It can be noted also that at a same ambient temperature a system with a higher mass vapour concentration has the higher interfacial temperature. In line with the negligible pressure deflect compared to the atmospheric pressure, all curves tend towards the boiling point at one atmospheric pressure ($T_i = 373.15$ K).

5. Concluding remarks

The evaporation of water by mixed and free convection where resultant forces of thermal and solutal buoyancies act in the downward direction in a vertical channel has been numerically studied for an air–water system. The effects of the ambient conditions of the humid air such as the temperature and the concentration on the heat and mass transfer in the flow are examined in detail. On the other hand, the effectiveness of the evaporation rate as function of the free stream temperature and vapour concentration is also studied.

A brief summary of the major results is as follows:

- For the mixed convection case, reducing the inlet gas velocity increases the secondary flow and disturbs the thermal and mass fields.
- The evaporation rate is independent on the free stream mass flux for the forced convection case. However, taking into account the buoyancy effects will change this behaviour.
- For the pure natural case, higher inlet flow rate is found to be associated with a larger inlet temperature or lower inlet concentration at a fixed free stream temperature.
- The existence of the inversion temperature observed previously in the case of forced convection flow is

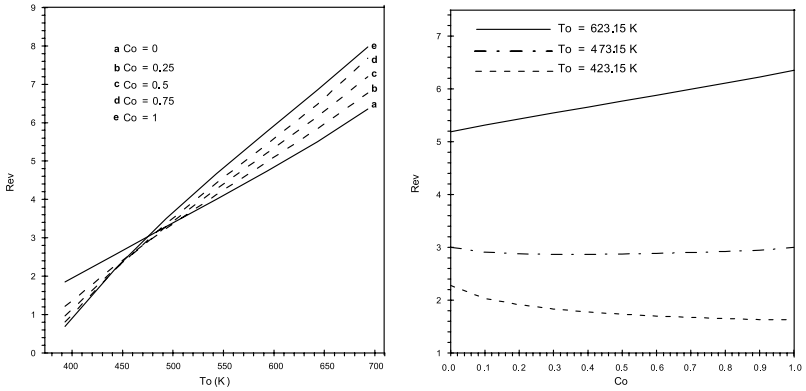

Fig. 12. Effect of ambient conditions of temperature and concentration on inlet evaporative rate ($T_w = 373.15$ K, $d/H = 0.05$, $p_0 = 1$ atm).

confirmed for the problem of mixed and natural convection. This temperature is defined as the intersection of the evaporation rate curves for dry air and superheated steam when plotted over gas inlet temperature. Based on the present results, we can conclude that inversion temperature values in the case of natural and mixed convection are nearly the same in the case of forced convection.

References

[1] L. Wenzel, R.R. White, Drying granular solids in superheated steam, Ind. Engng. Chem. 43 (1951) 1829–1851.

[2] J.C. Chu, A.M. Lane, D. Conklin, Evaporation of liquids into their superheated vapour, Ind. Engng. Chem. 45 (1953) 1586–1591.

[3] T. Yoshida, T. Hyõdõ, Evaporation of water in air humid air, and superheated steam, Ind. Engng. Chem. Process Des. Dev. 9 (1970) 207–214.

[4] L.C. Chow, J.N. Chung, Evaporation of water into laminar stream of air and superheated steam, Int. J. Heat Mass Transfer 26 (3) (1983) 373–380.

[5] C.H. Wu, D.C. Davids, J.N. Chung, Simulation of wedge-shaped product dehydration using mixtures mixture of superheated steam and air in laminar flow, Numer. Heat Transfer 11 (1987) 109–123.

[6] L.C. Chow, J.N. Chung, Water evaporation into a turbulent stream of air, humid air or superheated steam, in: Proceedings of the ASME National Heat Transfer Conference, ASME, No. 83-HT-2, New York, 1983.

[7] J.P. Schwartze, S. Bröcker, The evaporation of water into air of different humidities and the inversion temperature phenomenon, Int. J. Heat Mass Transfer 43 (2000) 1791–1800.

[8] M. Hassan, A.S. Mujumdar, M. Al-Taleb, Laminar evaporation from flat surface into unsaturated superheated solvent vapour. Drying 1986, Hemisphere (1986) 604–616.

[9] C.H. Wu, D.C. Davids, J.N. Chung, Simulated dehydration wedge-shaped specimens in turbulent flow of superheated steam and air, Drying Technol. 7 (4) (1989) 761–782.

[10] M. Haji, L.C. Chow, Experimental measurement of water evaporation rate into air and superheated steam, J. Heat Transfer 110 (1988) 237–242.

[11] R.K. Shah, A.L. London, Laminar Flow Forced Convection in Ducts, Academic Press, 1978.

[12] M.W. Kays, M.E. Crawford, Convective Heat and Mass transfer, Mc Graw Hill Book Company, 1980.

[13] Y.L. Tsay, T.F. Lin, W.M. Yan, Cooling of falling liquid film through interfacial heat and mass transfer, Int. J. Multiphase Flow 16 (5) (1990) 853–865.

[14] C.J. Chang, T.F. Lin, W.M. Yan, Natural convection flows in a vertical open tube resulting from combined buoyancy effects of thermal and mass diffusion, Int. J. Heat Mass Transfer 29 (10) (1986) 1543–1552.

[15] W.M. Yan, T.F. Lin, Combined heat and mass transfer in natural convection between vertical parallel plates with film evaporation, Int. J. Heat Mass Transfer 33 (3) (1990) 529–541.

[16] A. Missenard, Conductivités des solides, des liquides et des gaz, Edition Eyrolles, Paris, 1965.

[17] W.M. Yan, C.Y. Soong, Convective heat and mass transfer along an inclined heated plate with film evaporation, Int. J. Heat Mass Transfer 38 (7) (1995) 1261–1269.

[18] C. Debbissi, J. Orfi, S. Ben Nasrallah, Evaporation of water by free convection in a vertical channel including effects of wall radiative properties, Int. J. Heat Mass Transfer 44 (2001) 811–826.

[19] M.Vachon, Etude de l'évaporation en convection naturelle, Thèse de doctorat, Université de Poitiers, 1979.

[20] F.P. Incropera, D.P. Dewitt, Fundamentals of Heat and Mass Transfer, John Wiley and Sons, 1996.